J. Fluid Mech. (1992), *vol.* 239, *pp.* 341–358
Printed in Great Britain

Nonlinear analysis of flow in an elastic tube (artery): steady streaming effects

By D. M. WANG AND J. M. TARBELL

Department of Chemical Engineering, The Pennsylvania State University, 155 Fenske Laboratory, University Park, PA 16802, USA

(Received 29 October 1990 and in revised form 10 December 1991)

We analyse the nonlinear flow of a Newtonian fluid in an elastic tube when subjected to an oscillatory pressure gradient with motivation from the problem of blood flow in arteries. Two parameters: the unsteadiness, $\alpha = R_0(\omega/\nu)^{\frac{1}{2}}$ and the diameter variation, $\epsilon = (R_{\max} - R_0)/R_0$, are important in characterizing the flow problem. The diameter variation (ϵ) is taken to be small so that the perturbation method is valid, and asymptotic solutions for two limiting cases of the steady-streaming Reynolds number, $R_s = (\alpha\epsilon)^2$ (either small or large), are derived.

The results indicate that nonlinear convective acceleration induces finite mean pressure gradient and mean wall shear rate even when no mean flow occurs. The magnitude of this effect depends on the amplitude of the diameter variation and the flow rate waveforms and the phase angle difference between them, which can be related to the impedance (pressure/flow) phase angle. Changes in the impedance phase angle, which is indicative of the degree of wave reflection, can change the direction of the induced mean flow. It is also shown that the induced mean wall shear rate is proportional to α when α is large. In addition, it is observed that the steady flow structure in the core can be influenced by wave reflection. The streamlines in the core are always parallel to the tube wall when there is no reflection. However, with total reflection, the induced mean flow recirculates between the nodes and points of maximum amplitude in a closed streamline pattern. Implications of the steady-streaming phenomena for physiological flow applications are discussed in a concluding section.

1. Introduction

Fluid mechanics, particularly wall shear stress is believed by many to play an important role in vascular homeostasis and vascular disease (Ku *et al.* 1985; Nerem & Levesque 1987). Detailed knowledge of blood flow in large arteries is essential for understanding the influence of fluid mechanics on the arterial wall. To model flow behaviour in large arteries, Womersley (1955, 1957*a*) developed the linear theory of oscillatory flow in straight, isotropic, thin-walled, linearly elastic tubes by neglecting convective acceleration. In the present work, we shall concentrate on the nonlinear effects resulting from the convective acceleration. In addition, we will determine the role played by wave reflection in modulating the nonlinear effects.

Steady-streaming flow is an important nonlinear characteristic of oscillatory viscous flow. When a purely oscillatory viscous flow is set up over a curved surface, the Reynolds stresses associated with the nonlinear convective acceleration generate a steady streaming flow in the boundary layer, and the steady flow at the edge of the boundary layer can drive a mean flow in the inviscid core. Schlichting (1932) found

such flow when considering the small oscillations of a cylinder in a fluid at rest. The work of Riley (1965) and Stuart (1966) showed that the steady streaming could be characterized by the steady-streaming Reynolds number. When the steady-streaming Reynolds number is small, a simple Stokes-layer structure can describe the flow behaviour; while if the steady-streaming Reynolds number is large, a double boundary-layer scheme is required. Although they considered flow over a cylinder, their conclusions apply to any two-dimensional external flow problem. Riley (1975) reviewed several papers with regard to these kinds of flow phenomena. Merchant & Davis (1989) studied the problem in which the external free stream includes not only the purely oscillatory component but also a mean flow component.

Several other types of flow can generate steady streaming: oscillatory flow in tapered tubes (Hall 1974; Grotberg 1984), viscous flow in wave fields (Longuet-Higgins 1953), and oscillatory flow in wavy-walled channels (Nishimura *et al.* 1989). We are particularly interested in oscillatory flow with wall motion, a characteristic of physiological flow problems. Fung & Yih (1968) studied the nonlinear effects of peristaltic flow and concluded that the mean flow induced by the peristaltic motion of the wall is proportional to the square of wall movement amplitude. Secomb (1978) studied flow in a two-dimensional channel with pulsating walls and Padmanabham & Pedley (1987) considered the three-dimensional steady-streaming problem. These researchers have shown that in confined flow problems the mean vorticity stemming from the nonlinear convective acceleration is distributed over the entire cross-section and the steady streaming in the core should be described by the theory of inviscid rotational flow instead of by a double boundary-layer structure.

Womersley (1957*b*) calculated the first-order perturbation corrections for the nonlinear convective terms and concluded that the nonlinear effect on mean flow was not negligible. Ling & Atabek (1972), assuming that the local convective acceleration has a similar profile to the local velocity, carried out a nonlinear analysis of aortic flow using numerical methods. They analysed aortic flow data from dogs, and their results suggested that the convective acceleration might be important in the aorta. The numerical simulations reported by Dutta & Tarbell (1989) indicate that the steady-streaming flow in a straight elastic tube is dependent upon the phase angle between the pressure gradient and the wall motion. Recently, Dragon & Grotberg (1991) analysed mass transport in a flexible tube and proposed that the time-averaged mass transfer rate would be influenced by the existing steady-streaming flow.

In the present work, we determine the steady-streaming flow behaviour for the nonlinear Womersley problem. Assuming the wall motion is small (a realistic assumption in arteries), perturbation techniques are used to solve the weakly nonlinear version of the problem. We will discuss the effects of Womersley's unsteadiness parameter (α) and the steady-streaming Reynolds number (R_s). In addition, the influence of wave reflection will be taken into account. A similar approach was adopted by Womersley (1957*b*) and by Dragon & Grotberg (1991). But their solutions are only valid for small steady-streaming Reynolds number, and they did not consider the effects induced by wave reflections.

The problem is formulated in §2. Solutions for the case of arbitrary α but small R_s are presented in §3; and solutions for the case of large α, with R_s either small or large, are discussed in §4. In §5, the dependence of steady streaming on axial position along the tube is described and the role played by the wall property (tube law) is also discussed. In §6, the effects of the unsteadiness parameter, steady-streaming Reynolds number and wave reflection as characterized by the impedance phase angle

are discussed. Finally in §7, we compare the present work with that of others and discuss the physiological implications.

2. Formulation

We model blood flow in arteries using a homogeneous, incompressible Newtonian fluid in an isotropic, thin-walled, elastic tube with longitudinal constraint when the fluid is subjected to an oscillatory pressure gradient. The coupling of fluid motion and wall motion in general leads to a very difficult problem. However, by assuming the tube wall is elastic and that longitudinal wall motion is negligible, approximations which are quite reasonable for large arteries under normal flow conditions (Womersley 1957*a*; Ling & Atabek 1972), the equations describing wall motion can be simplified greatly, and we can concentrate on solving the nonlinear problem of fluid motion.

To describe axisymmetric flow in a tube, we choose the cylindrical coordinates r, θ and z, with z along the axis of the tube. The axial and radial velocities (W and U, respectively) are governed by the Navier–Stokes equations and the equation of continuity:

$$\frac{\partial W}{\partial t}+U\frac{\partial W}{\partial r}+W\frac{\partial W}{\partial z}=-\frac{1}{\rho}\frac{\partial P}{\partial z}+\nu\left(\frac{\partial^2 W}{\partial r^2}+\frac{1}{r}\frac{\partial W}{\partial r}+\frac{\partial^2 W}{\partial z^2}\right), \tag{2.1}$$

$$\frac{\partial U}{\partial t}+U\frac{\partial U}{\partial r}+W\frac{\partial U}{\partial z}=-\frac{1}{\rho}\frac{\partial P}{\partial r}+\nu\left(\frac{\partial^2 U}{\partial r^2}+\frac{1}{r}\frac{\partial U}{\partial r}-\frac{U}{r^2}+\frac{\partial^2 U}{\partial z^2}\right), \tag{2.2}$$

$$\frac{1}{r}\frac{\partial}{\partial r}(rU)+\frac{\partial W}{\partial z}=0. \tag{2.3}$$

The purely elastic wall motion can be described by the following constitutive equation:

$$\frac{R}{R_0}=a(P)=1+\tfrac{1}{2}\bar{D}\,(P-P_0)+\tfrac{1}{2}a''(P_0)\,(P-P_0)^2+\ldots. \tag{2.4}$$

We will develop travelling wave solutions in the z-direction subject to zero-slip boundary conditions assuming that there is no longitudinal wall motion. Hence, the boundary conditions are

$$\frac{\partial W}{\partial r}=0, \quad U=0 \quad \text{at} \quad r=0, \tag{2.5a}$$

$$W=0 \quad U=\frac{\partial R}{\partial t}, \quad \text{at} \quad r=R(t,z). \tag{2.5b}$$

In the above, t denotes time, P is the pressure, P_0 is the mean pressure, ρ is the density, ν is the kinematic viscosity, R is the tube radius, R_0 is the mean radius, and $\bar{D}$ is the distensibility of the tube wall.

We introduce non-dimensional variables and parameters as follows:

$$\tau=\omega t, \quad \hat{r}=\frac{r}{R_0}, \quad x=\frac{\omega z}{C_0}, \quad w=\frac{W}{C_0}, \quad u=\frac{U}{\omega R_0},$$

$$k=\frac{a''(p_0)}{\bar{D}^2}, \quad p=\frac{(P-P_0)}{\rho C_0^2}, \quad C_0=\frac{1}{(\rho_{\bar{D}})^{\frac{1}{2}}}, \quad \alpha=R_0(\omega/\nu)^{\frac{1}{2}},$$

where ω is the angular frequency, C_0 denotes the characteristic wave speed, and α is Womersley's unsteadiness parameter. Now dimensionless equations can be derived in terms of the above variables, and the dimensionless equations can be simplified by

making the long-wavelength approximation, $|\omega R_0/C_0| \ll 1$, which is realistic for arteries (Ling & Atabek 1972). Under this assumption, the axial viscous transport terms are negligible and (2.2) simply reduces to $\partial P/\partial r = 0$, indicating that the pressure is independent of radial position. However, the problem formulation is still awkward because of the moving boundary. To overcome this, we introduce a coordinate transformation $\xi = r/R(z,t)$. Then, the final dimensionless equations are

$$\frac{\partial w}{\partial \tau} = -\frac{\partial p(x,\tau)}{\partial x} + \frac{1}{\alpha^2}\frac{1}{a^2}\left(\frac{\partial^2 w}{\partial \xi^2} + \frac{1}{\xi}\frac{\partial w}{\partial \xi}\right) + \left(\frac{\xi}{a}\frac{\partial a}{\partial t} - \frac{u}{a}\right)\frac{\partial w}{\partial \xi} - w\left(\frac{\partial w}{\partial x} - \frac{\xi}{a}\frac{\partial w}{\partial \xi}\frac{\partial a}{\partial x}\right), \tag{2.6}$$

$$\frac{1}{\xi}\frac{\partial}{\partial \xi}(\xi u) + a\frac{\partial w}{\partial x} - \xi\frac{\partial a}{\partial x}\frac{\partial w}{\partial \xi} = 0, \tag{2.7}$$

$$a = 1 + \tfrac{1}{2}p + \frac{k}{2}p^2 + \ldots, \tag{2.8}$$

which are subject to the following boundary conditions:

$$\frac{\partial w}{\partial \xi} = 0, \quad u = 0 \quad \text{at} \quad \xi = 0, \tag{2.9a}$$

$$w = 0, \quad u = \frac{\partial a}{\partial \tau} \quad \text{at} \quad \xi = 1. \tag{2.9b}$$

These equations are nonlinear owing to the convective acceleration terms and therefore difficult to solve in general. But the diameter variation, $\epsilon\,(\equiv (R_{\max} - R_0)/R_0)$, in an artery is so small (typically 5–10 %) that perturbation methods can be used to attack the problem.

We consider the case of flow with purely sinusoidal flow rate at the input to the tube ($x = 0$) and no mean flow. Consequently, solutions of (2.6)–(2.9) will be sought in the following perturbation forms:

$$p = \epsilon p_{11} + \epsilon^2(p_{20} + p_{21} + p_{22}) + O(\epsilon^3), \tag{2.10a}$$

$$a = 1 + \epsilon a_{11} + \epsilon^2(a_{20} + a_{21} + a_{22}) + O(\epsilon^3), \tag{2.10b}$$

$$w = \epsilon w_{11} + \epsilon^2(w_{20} + w_{21} + w_{22}) + O(\epsilon^3), \tag{2.10c}$$

$$u = \epsilon u_{11} + \epsilon^2(u_{20} + u_{21} + u_{22}) + O(\epsilon^3), \tag{2.10d}$$

where p_{ij} represents the jth harmonic of the ith-order term in the expansion of p, with similar definitions for a_{ij}, w_{ij} and u_{ij}.

The solutions of $O(\epsilon)$ are those obtained by Womersley (1957*a*) for the linearized equations. In the present work, we will concentrate on the steady components of $O(\epsilon^2)$, w_{20} and u_{20}, which represent the main contributions to steady streaming. Our solution strategy is outlined below. Substituting (2.10) into (2.6), retaining terms up to $O(\epsilon^4)$, and taking the time average, we obtain

$$\frac{\epsilon^2}{\alpha^2}\left(\frac{\partial^2 w_{20}}{\partial \xi^2} + \frac{1}{\xi}\frac{\partial w_{20}}{\partial \xi}\right) - \epsilon^4\left(u_{20}\frac{\partial w_{20}}{\partial \xi} + w_{20}\frac{\partial w_{20}}{\partial x}\right) = \epsilon^2 h[\,], \tag{2.11}$$

where h [ ] represents a very complicated function containing terms of $O(\epsilon)$, $O(\epsilon^2)$, $O(\epsilon^3)$ and $O(\epsilon^4)$. The first term of (2.11) describes the viscous effects on the steady flow and the second term describes the corresponding steady convective effects. The steady-streaming Reynolds number, $R_s = \epsilon^2\alpha^2$, is defined as the ratio of the magnitudes of steady convective effects to the steady viscous effects (Riley 1965; Stuart 1966). When $R_s < O(1)$, the steady convective terms can be neglected and we need only solve the equations up to $O(\epsilon^2)$ to determine w_{20} and u_{20}. The solution

procedure for this case is described in §3. However, if $R_s \geqslant O(1)$ ($\alpha \geqslant O(1/\epsilon)$), an alternative approach is needed. Inside the Stokes layer, where the normalized distance to the wall is on the order of $1/\alpha$, the viscous term still dominates. But the steady convective term in the core is not negligible so that the steady component of the velocity profile cannot be determined until we evaluate the equations up to $O(\epsilon^4)$. The solution for R_s fixed as $\epsilon \to 0$, with the further limits $R_s \to 0$ and $R_s \to \infty$ will be discussed in §4. As we will show in §§3 and 4, the dependence of steady streaming on the axial position, x, and the radial coordinate, ξ, at $O(\epsilon^2)$ are separable for the cases we solve. In §§3 and 4, we determine the dependence on ξ and leave the dependence on x for §5 where the tube law is discussed.

3. Solution for arbitrary α and small R_s

Substituting (2.10) into (2.6)–(2.7) and (2.9) and equating coefficients of equal powers of ϵ, we obtain the equations and boundary conditions for the $O(\epsilon)$ and $O(\epsilon^2)$ problems.

$O(\epsilon)$ solution The periodic solution of the $O(\epsilon)$ problem is

$$p'_{11} = R\{f(x)\,e^{i\tau}\}, \quad a_{11} = R\{-\tfrac{1}{2}C_1^2 f'(x)\,e^{i\tau}\}, \tag{3.1a, b}$$

$$w_{11} = R\left\{if(x)\left(1-\frac{J_0(\alpha i^{\frac{3}{2}}\xi)}{J_0(\alpha i^{\frac{3}{2}}\xi)}\right)e^{i\tau}\right\}, \tag{3.1c}$$

$$u_{11} = R\left\{-if'(x)\left(\tfrac{1}{2}\xi-\frac{J_1(\alpha i^{\frac{3}{2}}\xi)}{\alpha i^{\frac{3}{2}}J_0(\alpha i^{\frac{3}{2}})}\right)e^{i\tau}\right\}, \tag{3.1d}$$

$$C_1^2 = 1-\frac{2J_1(\alpha i^{\frac{3}{2}})}{\alpha i^{\frac{3}{2}}J_0(\alpha i^{\frac{3}{2}})}, \tag{3.1e}$$

where $R\{\}$ denotes the real part of a complex variable and the prime indicates differentiation with respect to x. $f(x)$ is a function which describes the dependence of the flow rate on axial position at $O(\epsilon)$. It can be determined from the axial boundary conditions and the tube law, but at this moment we retain it as an unknown function.

Clearly, at $O(\epsilon)$ we have recovered Womersley's linear theory (Womersley 1957*a*) as expected. The second-order solution contains nonlinear interactions and will have both steady and oscillatory components. We will concentrate on the steady component and omit the oscillatory part in the present work.

$O(\epsilon^2)$ solution: steady-streaming effects The $O(\epsilon^2)$ equations for the steady-streaming component of the motion are

$$\frac{1}{\alpha^2}\left(\frac{\partial^2 w_{20}}{\partial\xi^2}+\frac{1}{\xi}\frac{\partial w_{20}}{\partial\xi}\right)-p'_{20}(x) = \overline{w_{11}\frac{\partial w_{11}}{\partial x}}-\overline{\left(\xi\frac{\partial a_{11}}{\partial\tau}-u_{11}\right)\frac{\partial w_{11}}{\partial\xi}}+\overline{\frac{2}{\alpha^2}a_{11}\left(\frac{\partial^2 w_{11}}{\partial\xi^2}+\frac{1}{\xi}\frac{\partial w_{11}}{\partial\xi}\right)}, \tag{3.2}$$

$$\frac{1}{\xi}\frac{\partial}{\partial\xi}(\xi u_{20})+\frac{\partial w_{20}}{\partial x} = \overline{\xi\frac{\partial a_{11}}{\partial x}\frac{\partial w_{11}}{\partial\xi}-a_{11}\frac{\partial w_{11}}{\partial x}}, \tag{3.3}$$

subject to

$$\frac{\partial w_{20}}{\partial\xi} = 0, \quad u_{20} = 0 \quad \text{at} \quad \xi = 0, \tag{3.4a}$$

$$w_{20} = 0, \quad u_{20} = 0 \quad \text{at} \quad \xi = 1, \tag{3.4b}$$

where $p'_{20}(x)$ represents the mean pressure gradient of $O(\epsilon^2)$ and an overbar denotes a time average.

Equations (3.2) and (3.3) can be transformed into a set of uncoupled non-

homogeneous ordinary differential equations. The solution procedure is straightforward, but the calculations are lengthy and complicated so they are omitted. The solution is

$$p'_{20}(x) = R\left\{F(x)\left[\frac{2\mathrm{i}}{C_1^2 C_1^{*2}} + \frac{3\mathrm{i}}{2} + \frac{1}{C_1^2}\left(\frac{11}{\alpha^2} - \frac{3\mathrm{i}}{2}\right) - \frac{1}{C_1^{*2}}\left(\frac{5}{\alpha^2} + \frac{3\mathrm{i}}{2}\right)\right]\right\}, \tag{3.5a}$$

$$w_{20} = R\{\tfrac{1}{4}\alpha^2(\xi^2-1)p'_{20}(x) + EF(x)\}, \tag{3.5b}$$

$$E = \frac{-\mathrm{i}\alpha^2}{8C_1^2 C_1^{*2}}(\xi^2-1) + \frac{\mathrm{i}\alpha^2}{4C_1^{*2}}\frac{\xi J_1(\alpha \mathrm{i}^{\frac{5}{2}}\xi) - J_1(\alpha \mathrm{i}^{\frac{5}{2}})}{\alpha \mathrm{i}^{\frac{5}{2}} J_0(\alpha \mathrm{i}^{\frac{5}{2}})} - \frac{\mathrm{i}\alpha^2}{4C_1^2 C_1^{*2}}\frac{\xi J_1(\alpha \mathrm{i}^{\frac{5}{2}}\xi) - J_1(\alpha \mathrm{i}^{\frac{5}{2}})}{\alpha \mathrm{i}^{\frac{5}{2}} J_0(\alpha \mathrm{i}^{\frac{5}{2}})}$$

$$- \frac{1}{C_1^2 C_1^{*2}}\frac{J_0(\alpha \mathrm{i}^{\frac{5}{2}}\xi) - J_0(\alpha \mathrm{i}^{\frac{5}{2}})}{J_0(\alpha \mathrm{i}^{\frac{5}{2}})} + \frac{1}{2C_1^2 C_1^{*2}}\frac{J_0(\alpha \mathrm{i}^{\frac{3}{2}}\xi) - J_0(\alpha \mathrm{i}^{\frac{3}{2}})}{J_0(\alpha \mathrm{i}^{\frac{3}{2}})}$$

$$- \frac{1}{2C_1^2 C_1^{*2}}\frac{\int_1^{\xi} \alpha \mathrm{i}^{\frac{5}{2}} J_0(\alpha \mathrm{i}^{\frac{3}{2}}\xi) J_1(\alpha \mathrm{i}^{\frac{5}{2}}\xi)\,\mathrm{d}\xi}{J_0(\alpha \mathrm{i}^{\frac{3}{2}}) J_0(\alpha \mathrm{i}^{\frac{5}{2}})}, \tag{3.5c}$$

$$F(x) = \mathrm{i}C_1^2 C_1^{*2} f'(x) f^*(x), \tag{3.5d}$$

where the asterisk denotes the complex conjugate.

The axial velocity profile in (3.5*b*) can be integrated and differentiated to determine the steady flow rate and the steady wall shear rate. Although the velocity profile is very complicated, the wall shear rate has the following simple form:

$$s_{20} = -\alpha^2 \epsilon^2 R\left\{F(x)\left[\frac{\mathrm{i}}{C_1^2 C_1^{*2}} + \frac{7\mathrm{i}}{8} + \frac{1}{C_1^2}\left(\frac{11}{2\alpha^2} - \mathrm{i}\right) - \frac{1}{C_1^{*2}}\left(\frac{5}{2\alpha^2} + \frac{7\mathrm{i}}{8}\right)\right]\right\}. \tag{3.6}$$

Here, s_{20} is the dimensionless mean wall shear rate (where the characteristic shear rate has been taken as C_0/R_0). The mean flow rate has been calculated by integration of the axial velocity profile and shown to be identically zero as required by the equation of continuity.

When no mean flow is imposed, the linear theory ($O(\epsilon)$ solution) predicts that the mean pressure gradient and mean wall shear rate are also zero. However, taking into account the nonlinear convective acceleration, we find that the mean pressure gradient, (3.5*a*), and the mean shear rate, (3.6), are not zero owing to steady streaming. The magnitude of these effects depends on α, ϵ and $F(x)$. In §5, we will show that $F(x)$ is an axial-coordinate-dependent complex function defined by the end conditions which may be interpreted in terms of wave reflection. The influence of these parameters on the steady-streaming phenomena will be explored in §6.

4. Solution for large α, small and large R_s

For large α, the flow field can be divided into two regions, the Stokes layer near the wall and the core. In the following analysis, we employ the original coordinate, ξ, to denote the radial position in the core. However, to examine the flow phenomena in the near-wall Stokes layer, which becomes very thin when α is large, we adopt the coordinate scale, $\eta = 1-\xi/(1/\alpha)$, where $1-\xi$ is the normalized distance from the wall and $1/\alpha$ is the normalized Stokes-layer thickness. This new coordinate transformation leads to different sets of equations for the Stokes layer and the core. These two regions can be matched by the asymptotic matching principle (Van Dyke 1964).

In this section, we shall seek asymptotic solutions in the limit $\alpha = O(\epsilon^{-1})$ ($R_s = O(1)$) as $\epsilon \to 0$, and then take further limits $R_s \to 0$ and $R_s \to \infty$ to solve the steady-streaming problem. A similar method has been used by Lyne (1970) to attack steady-streaming problems in curved pipes.

$O(\epsilon)$ *solution* Substituting (2.10) into (2.6)–(2.8) and then neglecting the viscous term because α is large, we obtain the $O(\epsilon)$ equations of the core. The $O(\epsilon)$ equations in the Stokes layer can be obtained by adopting the η coordinate scale and neglecting the higher-order terms. Afterwards, by matching the velocities at the edge of Stokes layer ($\xi \to 1$ and $\eta \to \infty$), we obtain the composite periodic solution at $O(\epsilon)$:

$$p'_{11}(x) = R\{\hat{f}(x)\,\mathrm{e}^{\mathrm{i}\tau}\}, \quad a_{11} = R\{-\tfrac{1}{2}\hat{f}'(x)\,\mathrm{e}^{\mathrm{i}\tau}\}, \tag{4.1a, b}$$

$$w_{11} = R\{\mathrm{i}[1-\exp(-\mathrm{i}^{\frac{1}{2}}\eta)]\,\hat{f}(x)\,\mathrm{e}^{\mathrm{i}\tau}\}, \quad u_{11} = R\{-\tfrac{1}{2}\mathrm{i}\xi\hat{f}'(x)\,\mathrm{e}^{\mathrm{i}\tau}\}, \tag{4.1c, d}$$

where $\hat{f}(x)$ is the large-α approximation of $f(x)$.

$O(\epsilon^2)$ *solution: steady-streaming effects in the boundary layer* Collecting all of the $O(\epsilon^2)$ terms and taking the time average leads to the governing equations for the steady-streaming component in the core and Stokes layer. The solution for the induced mean pressure gradient can be obtained by solving the $O(\epsilon^2)$ equations in the core, with the result

$$p'_{20}(x) = R\{\tfrac{1}{2}\mathrm{i}\hat{F}(x)\}, \tag{4.2}$$

$$\hat{F}(x) = \mathrm{i}\hat{f}'(x)\,\hat{f}^*(x). \tag{4.3}$$

By solving the time-averaged component of $O(\epsilon^2)$ in the Stokes layer, the steady-streaming components of the axial velocity in the Stokes layer can be determined and expressed as

$$w_{20} = R\{\hat{F}^*(x)\,[(1-\exp(-\mathrm{i}^{\frac{1}{2}}\eta))+\tfrac{1}{2}(\exp(\mathrm{i}^{\frac{3}{2}}\eta)-1)+\tfrac{1}{2}\mathrm{i}\,(\exp(-\mathrm{i}^{\frac{1}{2}}\eta)-1) + \tfrac{1}{4}(1+\mathrm{i})\,(\exp(-\sqrt{2}\eta)-1)]\}. \tag{4.4}$$

But the steady component of the velocity profile in the core cannot be determined until we evaluate the equations at $O(\epsilon^3)$ and $O(\epsilon^4)$.

$O(\epsilon^4)$ *solution: steady-streaming effects in the core* The solution for w_{11} in the core is not a function of ξ (see (4.1)) and neither are the solutions for w_{21} and w_{22} (which are omitted). Because of this, we can simplify the equation of $O(\epsilon^4)$ in the core and obtain the following time-averaged equation:

$$0 = -\frac{\partial p_{40}}{\partial x} + \frac{1}{R_s}\left(\frac{\partial^2 w_{20}}{\partial \xi^2} + \frac{1}{\xi}\frac{\partial w_{20}}{\partial \xi}\right) - u_{20}\frac{\partial w_{20}}{\partial \xi} - w_{20}\frac{\partial w_{20}}{\partial x} - \overline{w_{11}\frac{\partial w_{31}}{\partial x} + w_{31}\frac{\partial w_{11}}{\partial x} + w_{21}\frac{\partial w_{21}}{\partial x} + w_{22}\frac{\partial w_{22}}{\partial x}}. \tag{4.5}$$

Since this equation contains w_{31}, the following $O(\epsilon^3)$ equation must also be solved:

$$\frac{\partial w_{31}}{\partial t} = -\frac{\partial p_{31}}{\partial x} - w_{11}\frac{\partial w_{20}}{\partial x} - w_{20}\frac{\partial w_{11}}{\partial x}. \tag{4.6}$$

Using (4.6), w_{31} can be expressed as a function of p_{31} and w_{20} and then substituted into (4.5). Consequently, because p_{40}, p_{31}, w_{21} and w_{22} are not functions of ξ, we find that the steady flow in the core region is governed by the following equations:

$$\frac{1}{R_s}\left(\frac{\partial^2 w_s}{\partial \xi^2} + \frac{1}{\xi}\frac{\partial w_s}{\partial \xi}\right) - u_s\frac{\partial w_s}{\partial \xi} - w_s\frac{\partial w_s}{\partial x} = g(x), \tag{4.7}$$

$$\frac{1}{\xi}\frac{\partial}{\partial \xi}(\xi u_s) + \frac{\partial w_s}{\partial x} = 0, \tag{4.8}$$

subject to

$$\frac{\partial w_s}{\partial \xi} = 0, \quad u_s = 0 \quad \text{at} \quad \xi = 0, \tag{4.9a}$$

$$w_s = R\{\tfrac{3}{4}(1+\mathrm{i})\,\hat{F}(x)\}, \quad u_s = 0 \quad \text{at} \quad \xi = 1. \tag{4.9b}$$

The boundary conditions at $\xi = 1$ come from matching the core solution to the Stokes-layer solution. $g(x)$ is an arbitrary function chosen to satisfy

$$\frac{\partial}{\partial x}\left[\int_0^1 \xi w_s \, d\xi\right] = 0, \tag{4.10}$$

which stems from the conservation of mass and $w_s = w_{20} + R\{\frac{1}{2}\hat{F}(x)\}$.

Equations (4.7)–(4.10) can be solved analytically when R_s is either small or large. If R_s is small, $\epsilon \ll R_s \ll 1$, the solution can be expressed in terms of a stream function, ψ_s, as a power series in R_s:

$$\begin{aligned}\psi_s = {} & \tfrac{3}{8}(\xi^4 - \xi^2) R\{\hat{F}(x)(1+\mathrm{i})\} \\ & + R_s \tfrac{9}{16}(\tfrac{1}{144}\xi^7 - \tfrac{1}{48}\xi^5 + \tfrac{1}{48}\xi^3 - \tfrac{1}{144}\xi) R\{(1+\mathrm{i})\hat{F}(x)\} R\{(1+\mathrm{i})\hat{F}'(x)\} + O(R_s^2),\end{aligned} \tag{4.11}$$

where the steady stream function is defined as

$$w_s = \frac{1}{\xi}\frac{\partial \psi_s}{\partial \xi}, \quad u_s = -\frac{1}{\xi}\frac{\partial \psi_s}{\partial x}. \tag{4.12}$$

If $R_s \gg 1$, an approximate solution can be obtained by modifying Secomb's (1978) solution:

$$\psi_s = -\frac{3}{8\pi}\sin \pi\xi^2 R\{\hat{F}(x)(1+\mathrm{i})\}. \tag{4.13}$$

For the case of intermediate R_s, when both the viscous term and inertial terms are important, an analytical solution is not known.

The dimensionless wall shear rate can be calculated from the axial velocity profile, and for $R_s \ll 1$ the result is

$$s_{20} = \epsilon^2 R\{(-3 - 3\mathrm{i} - \tfrac{1}{4}\alpha(i)^{\frac{3}{2}})\hat{F}(x)\} \tag{4.14}$$

and for $R_s \gg 1$,

$$s_{20} = \epsilon^2 R\{-\tfrac{1}{4}\alpha(\mathrm{i})^{\frac{3}{2}}\hat{F}(x)\}. \tag{4.15}$$

5. The dependence on axial position and the tube law

According to (3.5), the axial dependence of steady-streaming effects is contained in the function $F(x)$. Once the $O(\epsilon)$ dependence of the flow rate on axial position is known ($f(x)$ in (3.1)), $F(x)$ can be determined through (3.5d). The dimensionless flow rate at $O(\epsilon)$, $q_1(x)$, can be expressed as

$$q_1(x) = R\{q(x)\,\mathrm{e}^{\mathrm{i}\beta(x)}\,\mathrm{e}^{\mathrm{i}\tau}\} = R\{\tfrac{1}{2}\mathrm{i}C_1^2 f(x)\,\mathrm{e}^{\mathrm{i}\tau}\}, \tag{5.1}$$

where q is the amplitude of the flow rate and β denotes the phase angle. Then $F(x)$ can be expressed as

$$F(x) = 2\left(\mathrm{i}\frac{\mathrm{d}q^2}{\mathrm{d}x} - 2q^2\frac{\mathrm{d}\beta}{\mathrm{d}x}\right). \tag{5.2}$$

The first term on the right-hand side of (5.2) is related to the change of flow rate amplitude, which depends on the existence of a reflected wave, and the second term is related to the variation of the phase angle. A similar structure was observed in the study of steady streaming due to oscillatory boundary layers (Batchelor 1967). We should point out that both the flow rate amplitude and phase angle may change with position along the aorta as a result of wave reflection from distal sites (Caro *et al.* 1978).

We can also interpret $F(x)$ in another way. Through (3.1b), the wall movement can be expressed as

$$a_{11} = R\{h(x)\,\mathrm{e}^{\mathrm{i}\gamma(x)}\,\mathrm{e}^{\mathrm{i}\tau}\} = R\{-\tfrac{1}{2}C_1^2 f'(x)\,\mathrm{e}^{\mathrm{i}\tau}\}, \tag{5.3}$$

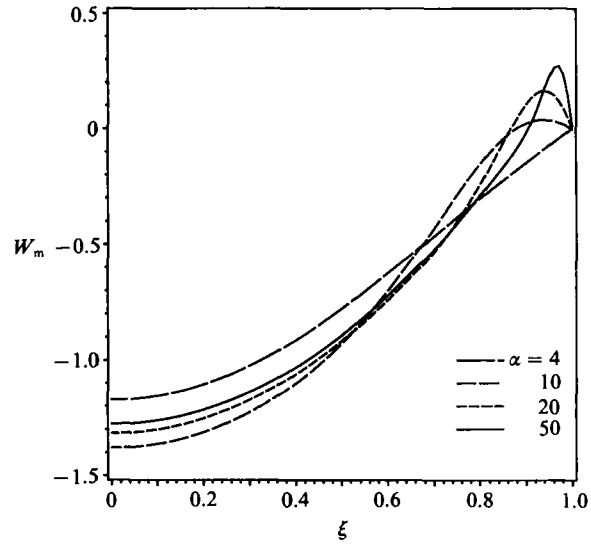

FIGURE 2. Dimensionless induced mean axial velocity profiles for different α at $\phi = 0°$. R_s is small.

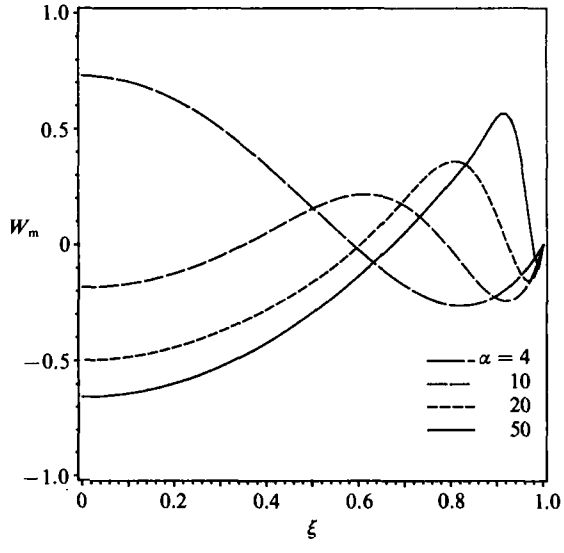

FIGURE 3. As figure 2 but at $\phi = -90°$.

where $E_r(\xi)$ and $E_1(\xi)$ are two real functions of ξ which can be determined from (3.5*a–c*). Consequently, the dimensional mean velocity is proportional to Q_1 and D, and depends on α and ϕ. The effect of α is depicted in figure 2 ($\phi = 0$) and figure 3 ($\phi = -90°$). The velocity profiles depend strongly on the unsteadiness parameter (α), especially in the region near the wall. The phase angle, ϕ, can also change the velocity profile dramatically as shown in figure 4 ($\alpha = 4$) and figure 5 ($\alpha = 20$). The flow near the wall can even change direction due to the change of ϕ (figure 5). It should be noted that for all cases depicted in figures 2–5, the induced mean flow rate at $O(\epsilon^2)$,

$$\int_0^1 \xi w_{20}\,\mathrm{d}\xi + \overline{2a_{11}} \int_0^1 \xi W_{11}\,\mathrm{d}\xi,$$

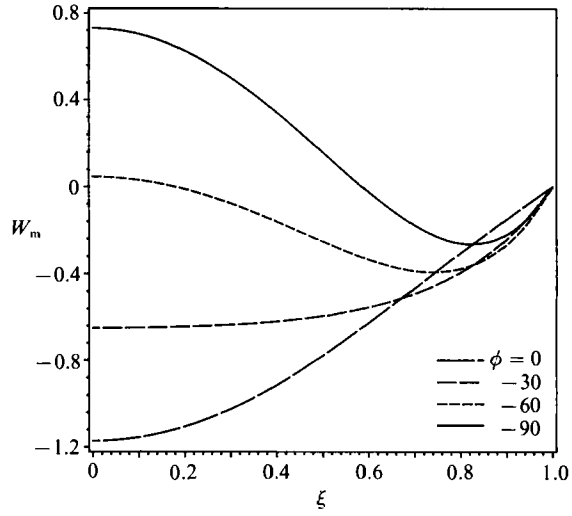

FIGURE 4. Dimensionless induced mean axial velocity profiles for different ϕ at $\alpha = 4$. R_s is small.

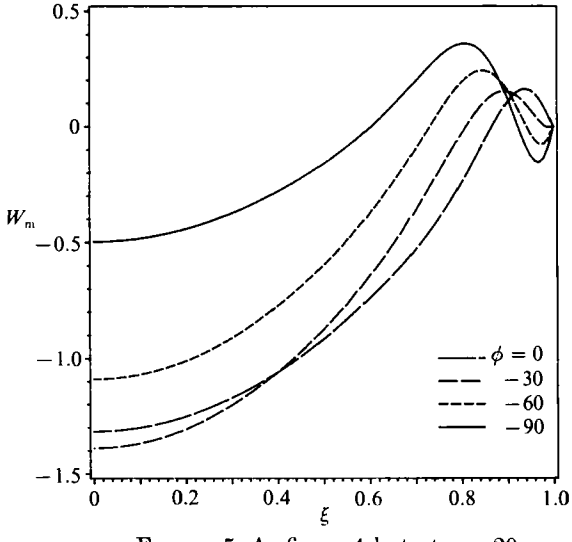

FIGURE 5. As figure 4 but at $\alpha = 20$.

is equal to zero (compare (4.10)). However, the integral of the induced mean velocity profile, $\int_0^1 \xi w_{20}\, d\xi$, is not zero.

For large α, the mean axial velocity profile in the Stokes layer is independent of R_s and is described by (4.4). The dependence of the mean velocity profile near the wall on the phase angle, ϕ, is shown in figure 6. It is interesting to note that the flow near the wall actually changes direction as ϕ crosses $-45°$.

Examination of (4.11) reveals that the mean axial velocity profile in the core is a parabolic function for small R_s (when $\alpha = O(\epsilon^{-1})$). This suggests that the induced mean flow in the core can be described by Poiseuille's equation with the wall moving in the direction opposite the pressure gradient (to match the flow at the edge of Stokes layer) for $R_s \ll 1$. On the other hand, for large R_s the mean axial velocity profile changes to $\cos \pi\xi^2$ because of the dominant steady convective terms. This is the same as Secomb's (1978) result.

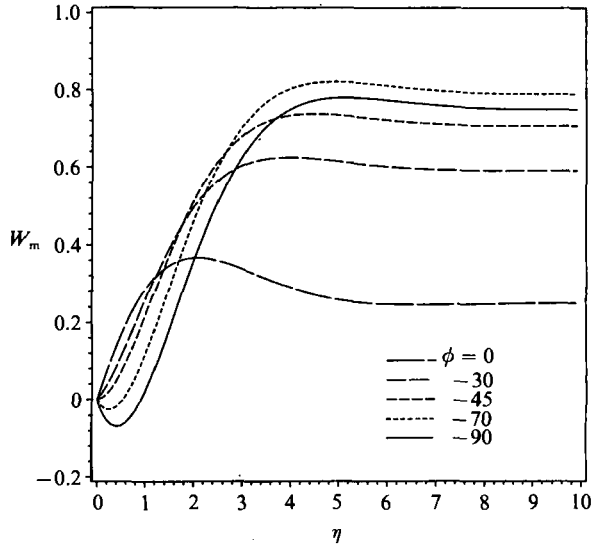

FIGURE 6. Dimensionless induced mean axial velocity profiles in the Stokes layer at different ϕ for large α. η is the normalized distance from the tube wall ($\eta = 0$ at the wall).

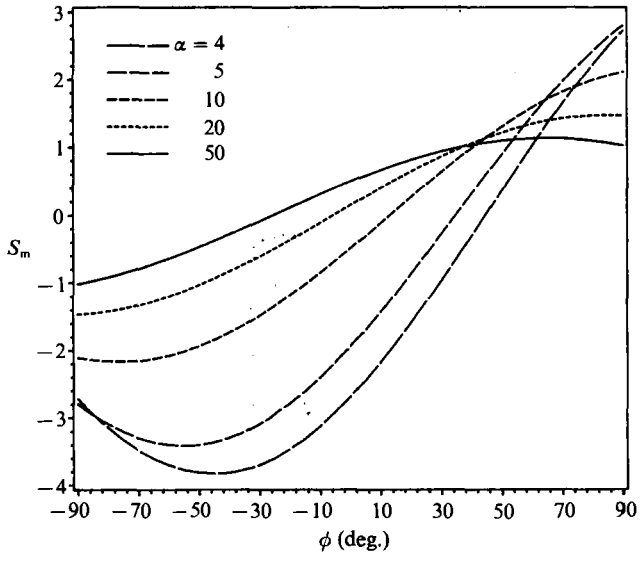

FIGURE 7. Dimensionless induced mean shear rate versus ϕ at different α. R_s is small.

We define the dimensionless mean wall shear rate as

$$S_m = \frac{4S_{20}\pi R_0^3}{\alpha Q_1 D}. \tag{6.5}$$

Making use of (6.1), we can rewrite (3.6) and express S_m as a function of α and ϕ. This relation is depicted in figure 7. The induced mean wall shear rate is proportional to the diameter variation and the oscillatory flow rate amplitude. The phase angle, ϕ, influences not only the magnitude of the induced mean wall shear rate but also the direction. For large α, the dimensionless induced mean wall shear rate (S_m) is

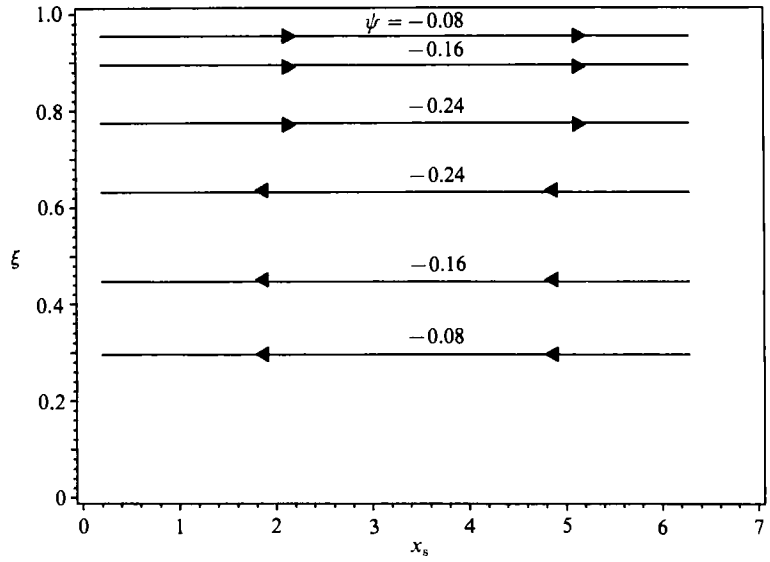

FIGURE 8. Streamlines in the core for large α but small R_s with no wave reflection. ξ and x_s are the dimensionless radial and axial coordinates respectively.

proportional to $\alpha \cos(-\phi+45°)$ (see (4.14) and (4.15)). Therefore, the induced mean wall shear rate may be significant when α is large, and its magnitude and direction are sensitive to ϕ.

Incorporating the tube law, (2.8), into (3.1) or (4.1), we find that the pressure variation (p_{11}) and the diameter variation (a_{11}) are in phase at $O(\epsilon)$. Hence, the phase angle, ϕ, can be interpreted as the phase angle difference between the pressure and flow, or the impedance (pressure/flow) phase angle. The impedance phase angle is a good indicator of the degree of wave reflection in a system. For large α, the impedance phase angle is zero everywhere along the tube when there is no wave reflection and is either 90° or $-90°$ when total reflection occurs. In addition, the 'telegraph line' equation (Taylor 1957) suggests that the oscillatory flow rate and diameter variation can be changed significantly by wave reflection. Consequently, the induced mean pressure gradient, the induced mean shear rate and the steady-streaming velocity profile can be modulated by wave reflections.

After examining (4.11), (4.13), and (5.7) we find that wave reflection can also change the steady flow structure in the core. For large α, the travelling wave always generates a steady flow in the wave propagation direction at the edge of the core and induces flow in the opposite direction near the centre region when there is no reflection (figure 8). However, the standing wave associated with total reflection induces a steady flow circulating between the nodes and the points of maximum amplitude (figure 9). The flow direction at the edge of the core is from the point of maximum amplitude to the node and the fluid near the centre flows in the reverse direction (for large α). The solutions for both large and small R_s suggest the same circulation structure, and similar results have been observed in Kundt's dust experiment (Schlichting 1979) and oscillatory viscous flow in wavy walled channels (Nishimura *et al.* 1989). For intermediate wave reflection the steady flow structure is a combination of these two structures (parallel and vortex).

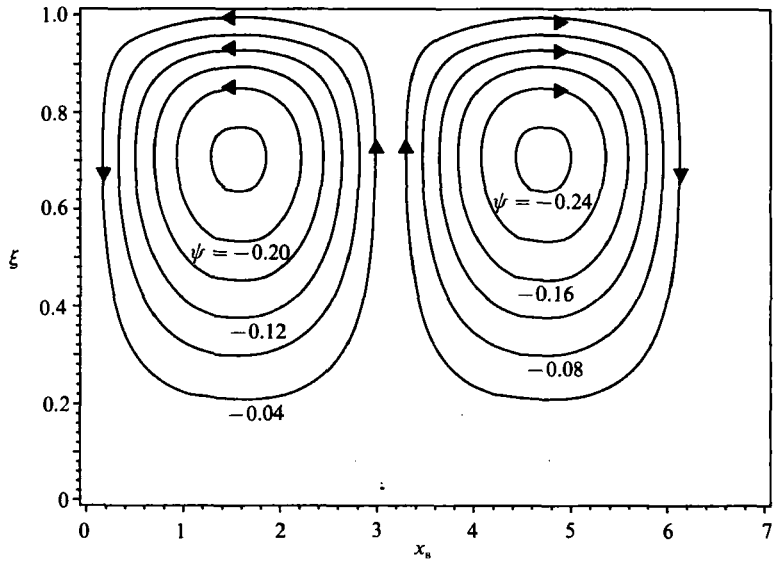

FIGURE 9. Streamlines in the core for large α but small R_s with total reflection. Nodes are at $x_s = 0$ and 2π, while maximum amplitude occurs at $x_s = \pi$.

7. Discussion

According to the analysis in §4, the steady-streaming flow scheme at high α in a distensible tube with a travelling wave is similar to the one discussed by Secomb (1978). Actually there is a simple relationship between Secomb's work and ours. If we consider the case of total wave reflection with its associated standing wave and analyse the flow near the node point, assuming the wavelength is much greater than the length of the tube, the matching boundary condition given by (4.9*b*) can be approximated as

$$w_s = -\tfrac{3}{2}(A_{11}^* B_{11} + A_{11} B_{11}^*)x \quad \text{at} \quad \xi = 1. \tag{7.1}$$

Hence, we can take a solution of the form $w_s = \hat{w}(\xi)x$, and the streaming equations of the core ((4.7) and (4.8)) can be reduced exactly to those obtained by Secomb assuming that the wall motion is independent of axial distance. This is valid only if the wavelength is much greater than the length of the tube. It should also be noted that Secomb implicitly included a node point because no flow could cross the symmetrical plane $x = 0$. Clearly then, Secomb's solution is a special case of the present work which describes steady-streaming phenomena when the wave propagates along the tube.

The generation of mean pressure gradient and mean wall shear rate, modulated by wave reflection, is the most important characteristic of steady streaming in a distensible tube. The relevance of these phenomena to blood flow in the aorta is discussed below.

In general, the mean pressure gradient applied to an oscillatory tube flow is balanced by the mean convective acceleration terms and the mean viscous terms. In a rigid straight tube, the nonlinear convective terms are negligible except near the entrance. However, this is not true for a flexible tube. In fact, when α is large, the mean convective acceleration terms can be larger than the mean viscous terms down the length of a flexible tube. In addition, the induction of mean pressure gradient is enhanced by wave reflection. This indicates that one cannot calculate the mean flow

rate or mean wall shear rate directly from the mean pressure gradient by Poiseuille's equation, as a physiologist would want to do, without considering the convective acceleration, particularly when wave reflection is important.

An induced mean velocity profile is generated due to the nonlinear convective acceleration. The dimensionless induced mean velocity ($O(\epsilon^2)$) is small compared to the imposed flow ($O(\epsilon)$). However, the dimensionless mean velocity, w_{20}, changes from zero (no slip on the wall) to $O(\epsilon^2)$ within a very thin Stokes layer (large α). Since the characteristic Stokes-layer thickness is on the order of $1/\alpha$, the dimensionless induced mean wall shear rate is on the order of $\alpha\epsilon^2$. If a mean flow, $O(\epsilon)$, is imposed, the imposed dimensionless mean wall shear rate is also on the order of ϵ according to Poiseuille's equation. In this case, the ratio of the induced mean wall shear rate to the imposed mean wall shear rate is on the order of $\alpha\epsilon$.

To obtain a sense of the magnitude of the induced mean wall shear rate in the aorta ($f = 1$ Hz), we take a typical aortic flow case for which $\alpha = 20$, DV = 10% and Q_1 (first-harmonic flow amplitude) = 15 l/min. For these parameters, the difference in the induced mean wall shear rate between $\phi = 0$ and $\phi = -90°$ (no wave reflection and total reflection, respectively) is equivalent to the wall shear rate, generated by a Poiseuille flow, of 3.6 l/min, about one quarter of the oscillatory flow rate and of the magnitude of the mean cardiac output. Thus it appears to be a significant effect in the aorta.

For large α, the induction of mean wall shear rate is proportional to $\alpha\cos(-\phi+45°)$. The range of the first-harmonic impedance phase angle *in vivo* is usually between 0° and −90° (McDonald 1974). As a result, the induction is positive in the range of 0 to −45°, negative in the range −45° to −90°, and changes sign when the impedance phase angle crosses −45°. Therefore, increased wave reflection is expected to diminish the mean wall shear rate. It is interesting to note in this context that the impedance phase angle of hypertensive patients is closer to −90° than in normal patients (Merillon *et al.* 1982). The present theory indicates that the mean wall shear rate would be reduced in hypertensive patients relative to normal. Since low (or oscillatory) mean wall shear stress appears to be the fluid mechanical factor which best correlates with the localization of atherosclerotic plaques in branching arteries (Ku *et al.* 1985), our results suggest an indirect mechanism for the role of hypertension in arterial disease: hypertension → increased wave reflection → reduced mean wall shear stress.

Wave reflection may also influence mass transport to the walls of the tube (artery) because of its effect on the mean flow pattern. The mean flow streamlines are parallel to the wall of the tube in the absence of wave reflection (figure 8), but a closed streamline circulation structure arises with total reflection (figure 9). Increased wave reflection will have the tendency to prolong the residence time of material in the circulation structure thus allowing more time for diffusive transport to the wall. In addition, the mean radial velocity is zero throughout the flow field in the absence of reflection (figure 8), but becomes more significant as wave reflection increases (figure 9). Since the mean radial velocity can affect mass transport to the vessel wall via convection, this mechanism of mass transfer may also be affected by wave reflection.

Further to the physiological relevance of this work, it must be remembered that owing to mathematical difficulties, we have only considered the case of oscillatory flow with zero mean flow rate. But the mean flow rate is not negligible *in vivo*. For small R_s, we can obtain the complete mean flow solution by simply adding the imposed mean flow field, which can be described by Poiseuille's equation, to the induced mean flow field, as described in the present paper. This has been assumed

implicitly in the discussion of the preceding paragraphs. But for $R_s \geqslant O(1)$, the imposed mean flow field is influenced by the oscillatory flow so that Poiseuille's equation cannot be used. However, the mean flow rate is of the same order of magnitude as the oscillatory flow rate in arteries, and the solution for this situation still remains as a challenge.

This work was supported by PHS Grant R01-H35549. We are grateful to Professor T. J. Pedley for his valuable advice.

REFERENCES

BATCHELOR, G. K. 1967 *An Introduction to Fluid Dynamics.* Cambridge University Press.

CARO, C. G., PEDLEY, T. J., SCHROTER, R. C. & SEED, W. A. 1978 *The Mechanics of the Circulation.* Oxford University Press.

DRAGON, G. A. & GROTBERG, J. B. 1991 Oscillatory flow and mass transport in a flexible tube. *J. Fluid Mech.* **231**, 135–155.

DUTTA, A. & TARBELL, J. M. 1989 Numerical simulation of sinusoidal flow in a straight elastic tube: effects of phase angles. *Biorheol.* **26**, 1–22.

FUNG, Y. C. & YIH, C. S. 1968 Peristaltic transport. *Trans. ASME* E: *J. Appl. Mech.* **35**, 669–675.

GROTBERG, J. B. 1984 Volume-cycled oscillatory flow in a tapered channel. *J. Fluid Mech.* **141**, 249–264.

HALL, P. 1974 Unsteady viscous flow in a pipe of slowly varying cross-section. *J. Fluid Mech.* **64**, 209–226.

KU, D. N., GIDDENS, D. P., ZARINS, C. K. & GLAGOV, S. 1985 Pulsatile flow and atherosclerosis in the human carotid bifurcation. *Arteriosclerosis* **5**, 293–302.

LING, S. C. & ATABEK, H. B. 1972 A nonlinear analysis of pulsatile flow in arteries. *J. Fluid Mech.* **55**, 493–511.

LONGUET-HIGGINS, M. S. 1953 Mass transport in water waves. *Phil. Trans. R. Soc. Lond.* A **245**, 535–581.

MCDONALD, W. A. 1974 *Blood Flow in Arteries.* Baltimore: Williams and Wilkins Co.

MERCANT, G. J. & DAVIS, S. H. 1989 Modulated stagnation-point flow and steady streaming. *J. Fluid Mech.* **198**, 543–555.

MERILLON, J. P., FONTENIER, G. J., LERALLUT, J. F., JAFFRIN, M. Y., MOTTE, G. A., GENAIN, C. P. & GOURGON, R. R. 1982 Aortic input impedance in normal man and arterial hypertension: Its modifications during changes in aortic pressure. *Cardiovasc. Res.* **16**, 646–656.

NEREM, R. M. & LEVESQUE, M. J. 1987 In *Handbook of Bioengineering*, pp. 21.1–21.22. McGraw-Hill.

NISHIMURA, T., ARAKAWA, S., MURAKAMI, S. & KAWAMURA, Y. 1989 Oscillatory viscous flow in symmetric wavy-walled channels. *Chem. Eng. Sci.* **44**, 2137–2148.

PADMANABHAN, N. & PEDLEY, T. J. 1987 Three-dimensional steady streaming in a uniform tube with an oscillating elliptical cross-section. *J. Fluid Mech.* **178**, 325–343.

RILEY, N. 1965 Oscillating viscous flows. *Mathematika* **12**, 161–175.

RILEY, N. 1975 Unsteady laminar boundary layers. *SIAM Rev.* **17**, 274–297.

SCHLICHTING, H. 1932 Berechnung Ebener Periodischer Grenzschichtstromungen. *Phys. Z.* **33**, 327–335.

SCHLICHTING, H. 1979 *Boundary Layer Theory*, Ch. 15, pp. 431–432. McGraw-Hill.

SECOMB, T. W. 1978 Flow in a channel with pulsating walls. *J. Fluid Mech.* **8**, 273–288.

STUART, J. T. 1966 Double boundary layers in oscillatory flow. *J. Fluid Mech.* **24**, 673–687.

TAYLOR, M. G. 1957 An approach to an analysis of the arterial pulse wave – I. Oscillations in an attenuating line. *Phys. Med. Biol.* **1**, 258–269.

VAN DYKE, M. 1964 *Perturbation Methods in Fluid Mechanics.* Academic.

WOMERSLEY, J. R. 1955 Oscillatory motion of a viscous liquid in a thin-walled elastic tube – I. The linear approximation for long waves. *Phil. Mag.* (7) **46**, 199–221.

WOMERSLEY, J. R. 1957*a* Oscillatory flow in arteries: the constrained elastic tube as a model of arterial flow and pulse transmission. *Phys. Med. Biol.* **2**, 178–187.

WOMERSLEY, J. R. 1957*b* An elastic tube theory of pulse transmission and oscillatory flow in mammalian arteries. *WADC Tech. Rep.* 56–614.